
Article:
Patterson, Anna, El-Qarra, Lamisse and Smith, David Kelham orcid.org/0000-0002-9881-2714 (2022) Chirality-directed hydrogel assembly and interactions with enantiomers of an active pharmaceutical ingredient. Chemical communications. pp. 3941-3944. ISSN: 1364-548X

https://doi.org/10.1039/d1cc06942j

ChemComm

COMMUNICATION

View Article Online
View Journal | View Issue

Cite this: *Chem. Commun.*, 2022, **58**, 3941

Received 9th December 2021,
Accepted 1st March 2022

DOI: 10.1039/d1cc06942j

rsc.li/chemcomm

Chirality-directed hydrogel assembly and interactions with enantiomers of an active pharmaceutical ingredient†

Anna K. Patterson, Lamisse H. El-Qarra and David K. Smith *

Enantiomers of the low-molecular-weight gelator (LMWG) DBS-CONHNH$_2$, based on D- or L- 1,3 : 2,4-dibenzylidenesorbitol (DBS), were synthesised. Enantiomeric gels are equivalent, but when mixtures of enantiomers are used, although gels still form, they are weaker than homochiral gels. Nanoscale chirality is lost on adding even a small proportion of the opposite enantiomer – homochiral assembly underpins effective gelation. Enantiomeric gels encapsulate the two enantiomers of anti-inflammatory drug naproxen, with thermal & mechanical differences between diastereomeric systems. We hence demonstrate the importance of chirality in DBS assembly and its interactions with chiral additives.

Many hydrogels self-assembled from low-molecular-weight gelators (LMWGs) are based on molecules that occur naturally and contain chiral centres.[1] Although enantiomeric gelators give rise to gels with equivalent physical properties, gelator chirality can impact on the chirality of the self-assembled nanostructures.[2] When enantiomers are combined, there are a number of possible outcomes. If homochiral interactions are favoured, there may be self-sorting, with enantiomers forming separate homochiral assemblies.[3] If heterochiral interactions are preferred, then the gelators may form a true-racemate, being arranged in an alternating pattern.[4] Alternatively, there may be little difference in interaction between enantiomers, giving rise to a pseudo-racemate, with randomly mixed gelators – this often prevents gelation,[5] but occasionally, a gel is still formed.[6] In addition to fundamental interest in chiral gels, there is increasing interest in the impact of chirality on applications.[7] In tissue engineering, Feng and co-workers showed that cell adhesion can be controlled by changing LMWG chirality.[8] In drug delivery, Xu and co-workers demonstrated the greater resistance of D-peptide gels to proteolytic enzymes, enhancing stability.[9] Enantiomeric gels can also be proficient in asymmetric catalysis,[10] and their ability to perform enantioselective recognition is a topic of burgeoning interest.[11,12]

Gels based on 1,3;2,4-dibenzylidenesorbitol have been used for some years in industry, and new derivatives are being explored in an academic setting for high-tech use.[13] Previously, D-DBS (based on naturally-abundant D-sorbitol) has been compared to a racemic mixture of D- and L-DBS, with the mixture found to be incapable of forming organogels.[14] In terms of DBS derivatives, studies to date have all used D-sorbitol. For example, D-DBS-CONHNH$_2$ hydrogels (Fig. 1) have been investigated in (*e.g.*) drug delivery and tissue engineering.[15] In such uses, bulk quantities are not necessarily required, and gelators based on L-sorbitol may offer advantages whilst still being commercially viable. We therefore decided to synthesise L-DBS-CONHNH$_2$, and explore the effects of chirality on self-assembly. We also explored the impact of chirality on formulation with naproxen (Fig. 1), a chiral active pharmaceutical ingredient (API).[16]

Firstly, L-DBS-CO$_2$Me was synthesised using the method previously reported for D-DBS-CO$_2$Me,[17] simply replacing D-sorbitol in the first step with L-sorbitol. It was converted to L-DBS-CONHNH$_2$ using hydrazine monohydrate in the same way as the D-enantiomer.[15a] The desired products were obtained in good yield with NMR, IR and MS characterisation in agreement with that reported for the D enantiomers.

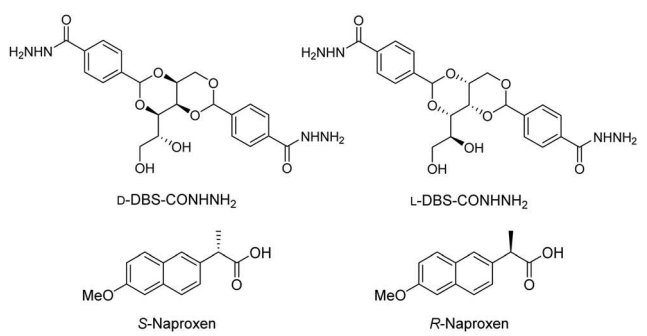

Fig. 1 Structures of D- and L-DBS-CONHNH$_2$ and *S*- and *R*-Naproxen.

Department of Chemistry, University of York, Heslington, York, YO10 5DD, UK. E-mail: david.smith@york.ac.uk

† Electronic supplementary information (ESI) available. See DOI: 10.1039/d1cc06942j

L-DBS-CONHNH$_2$ was tested for gelation by adding known amounts to sample vials with deionised water (0.5 ml). Samples were sonicated for 15 min before the solid was fully dissolved by heating. The resulting solution was left to cool, then gelation tested by tube inversion. As expected, the two enantiomers had the same ability to form hydrogels, with the same minimum gelation concentration (MGC) of 0.20% wt/vol (Table S1, ESI†). The T_{gel} values for enantiomeric gels were very similar (Table S2). Parallel plate rheology at a loading of 0.28% wt/vol (Fig. S1 and S2, ESI†) indicated that G' values in the LVR are also very similar, *i.e.*, the enantiomeric hydrogels have equivalent stiffnesses. The two gels also have very similar G'/G'' crossover points (*ca.* 8% strain).

To understand the nanoscale behaviour of the enantiomeric gels, electron microscopy was carried out. Although drying effects can impact on such images,[18] this remains an effective method for comparing gels from related gelators prepared in equivalent ways. SEM imaging (Fig. S3, ESI†) indicated both enantiomers form highly branched networks of nanoscale fibres (*ca.* 30 nm diameter). TEM imaging revealed the helical/twisted nature of the fibres formed (Fig. S4 (ESI†) and Fig. 3B). However, the handedness could not easily be determined as there appear to be left and right handed helical grooves equally spaced on the fibres, making it impossible to determine a twist direction. The two enantiomers give similar morphologies. This is as expected – the only change would be in the handedness, which cannot be determined here.

Variable temperature circular dichroism (VT-CD) spectroscopy is perhaps the most useful tool for observing chiral nanostructure assembly. Samples of the two enantiomers were prepared at a concentration of 0.10% wt/vol – although this is below the MGC, samples prepared at higher loadings were too concentrated to give useful spectra due to lack of transparency. The loading is only just below the MGC, and as such, there is still sufficient gelator for nanostructures to assemble, albeit they cannot fully establish a sample-spanning gel network. The UV spectrum of DBS-CONHNH$_2$ has a band at 252 nm due to the aromatic wings (Fig. S10). Both enantiomers had CD bands at *ca.* 272 nm and 235 nm (Fig. 2) consistent with the organisation of the aromatic wings in a local chiral microenvironment. On raising temperature, the CD bands change intensity, with that at 272 nm getting smaller and that at 235 nm getting larger, suggesting the former is associated with self-assembled gelator and the latter with individual dissolved gelator molecules. The biggest change in ellipticity, suggestive of disassembly, occurred between 75 °C and 85 °C – in line with the T_{gel} values. Importantly, the CD spectra observed for D- and L-DBS-CONHNH$_2$ were equal and opposite in ellipticity, reflecting the enantiomeric relationship.

We then explored the assembly of mixtures of enantiomers. Different ratios of D-DBS-CONHNH$_2$ and L-DBS-CONHNH$_2$ were investigated by mixing a known mass of each gelator in ratios ranging from 100 : 0 to 0 : 100 in units of 10, keeping the total concentration of gelator constant at 0.28% wt/vol. The samples were sonicated, then heated until all of the solid was dissolved. Once the samples had cooled, gelation was tested *via* tube inversion. In all cases a gel was formed (Table S3, ESI†). This was in contrast to previous reports for unmodified DBS,[14] in which mixing enantiomers prevented gelation. For all mixtures, the T_{gel} value was significantly lower (Table S4, ESI†) than for the homochiral hydrogels (*ca.* 100 °C at this concentration, Fig. 3A, blue). This indicates the enantiomers somewhat disrupt one another's assembly, resulting in a less thermally-stable network. Interestingly, there were no significant differences depending on the precise ratio of enantiomers, suggesting even a small amount of the 'wrong' enantiomer disturbs assembly and a new gel structure results.

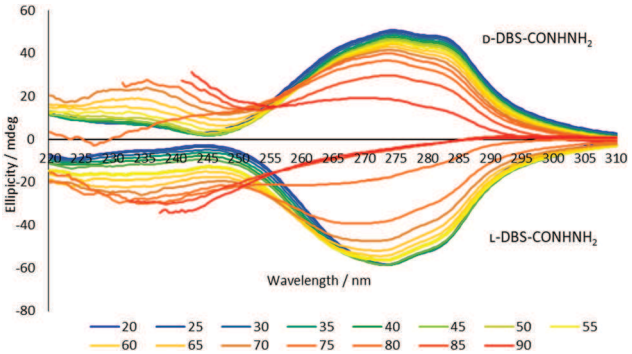

Fig. 2 Variable temperature circular dichroism spectroscopy (VT-CD) of D-DBS-CONHNH$_2$ and L-DBS-CONHNH$_2$ in H$_2$O at a loading of 0.10% wt/vol.

Rheology was performed on mixed D-DBS-CONHNH$_2$: L-DBS-CONHNH$_2$ hydrogels, with 50 : 50, 25 : 75 and 75 : 25 ratios (Fig. S5, S6 and Table S5, ESI†). These were compared with samples of the pure enantiomers. The 50 : 50 mix had a G' value of *ca.* 230 Pa – considerably lower than the value of *ca.* 600 Pa for pure L-DBS-CONHNH$_2$ (Fig. 3A, red). This is further evidence that interactions between enantiomers are disruptive, leading to softer gels. However, the interactions are not sufficiently disrupted to prevent gel assembly, as evidenced by the clear LVR. The 25 : 75 and 75 : 25 mixtures also showed drops in G', indicating a smaller amount of the 'wrong' enantiomer also leads to softer hydrogels.

A ^{1}H NMR study was used to determine if mixing resulted in less gelator being incorporated into the gel network. When standard ^{1}H NMR spectroscopy is carried out on a gel, any gelator incorporated into the 'solid-like' gel network will not appear in the spectrum.[19] With an internal standard, 'mobile' gelator can be quantified. Comparing L-DBS-CONHNH$_2$ and a 50 : 50 mixture of L-DBS-CONHNH$_2$ and D-DBS-CONHNH$_2$, we found that in both cases, very little 'free' gelator was visible (Fig. S7, ESI†). For L-DBS-CONHNH$_2$, only 1.5% of total gelator was visible. For the racemic gel, this value was 3.6%. Although the racemic gel has slightly more free gelator, most has nonetheless assembled. This indicates that, even though the gel is weaker, the vast majority of both enantiomers still assemble into a 'solid-like' network even when mixed.

SEM imaging of the 50 : 50 system indicates the racemic gel has a branched sample-spanning self-assembled network similar to L-DBS-CONHNH$_2$ alone (Fig. S8, ESI†). TEM images (Fig. S9, ESI†),

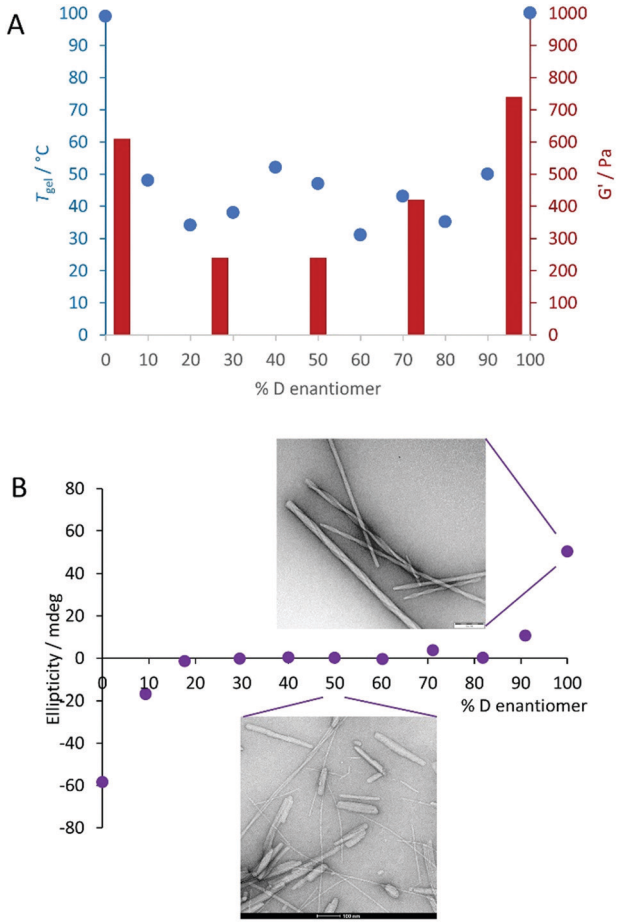

Fig. 3 (A) Thermal (blue) and rheological (red) data for the gels based on mixtures of D-DBS-CONHNH$_2$ and L-DBS-CONHNH$_2$ in H_2O at total loadings of 0.28% wt/vol. (B) CD data (purple) for the gels based on mixtures of D-DBS-CONHNH$_2$ and L-DBS-CONHNH$_2$ in H_2O at total loadings of 0.10% wt/vol, and selected TEM images representing 100% D-DBS-CONHNH$_2$ (top) and 50/50 L/D-DBS-CONHNH$_2$ (bottom). Further SEM images can be found in the ESI.†

however, are quite different – with fibres appearing both narrower and wider, but significantly more fragmented in the racemic mixture (Fig. 3B, bottom) than in the single enantiomer gel (Fig. 3B top). This lack of homogeneity explains the reduced thermal stability and mechanical strength of the racemic gel. This clearly indicates that the 50 : 50 mix has a less well-defined self-assembly mode.

FT-IR on the dried xerogels provided further insight. As expected, the two enantiomers had identical IR spectra (Fig. S14 and S15, ESI†). A 50 : 50 mixture of enantiomers was almost identical to the individual enantiomers, but the O–H stretch at *ca.* 3183 cm^{-1} shifted to 3193 cm^{-1} (Fig. S16, ESI†). This suggests a stronger O–H bond, indicating weaker hydrogen bonds on mixing enantiomers, which would explain the disruptive effect. However, it should be noted the IR shift is small, and the peaks broad, so care should be taken in interpreting these data.

Mixtures of enantiomers were investigated by CD, using a total gelator loading of 0.10% wt/vol. On addition of even a small proportion of the opposite enantiomer, the CD ellipticity dropped dramatically, indicating the nanoscale chirality of the self-assembled objects was almost completely lost (Fig. 3B, purple). At a 90 : 10 ratio, the ellipticity fell from *ca.* ±60 mdeg for the pure enantiomer to only *ca.* ±20 mdeg. Once 20% of the mixture is the 'wrong' enantiomer, the ellipticity is completely lost. Interactions between the two enantiomers therefore result in achiral nanostructures – even when only a small proportion of the total gelator is the 'wrong' enantiomer. This is in-line with the observation that even a small amount of the opposite enantiomer leads to a decrease in gel thermal stability and stiffness, and supports the TEM observation that different nanostructures are formed by the racemic system.

These results can be related to unfunctionalised DBS,[14] in which mixing enantiomers also disrupts assembly – but in the case of DBS gel formation is completely lost. Unfunctionalised DBS, which forms gels in organic solvents, relies primarily on hydrogen bonding between sorbitol backbone O-H groups to drive self-assembly – they must therefore be optimally aligned. However, DBS-CONHNH$_2$ forms gels in water, and hydrophobic effects can help drive self-assembly even in the absence of perfect alignment of hydrogen bonding O-H groups, potentially making it more tolerant of chiral mismatching. Simulation supports the lesser importance of H-bonding in DBS-CONHNH$_2$ assembly compared with unfunctionalized DBS.[20]

Many bioactive molecules have one or more chiral centres. Naproxen (NPX) is a non-steroidal anti-inflammatory drug, with the *S* form being both more effective and less toxic than the *R* form.[16] The drug is used as a single enantiomer, but other drugs in the same class (*e.g.* ibuprofen, ketoprofen *etc.*) are used as racemic mixtures. In previous work, D-DBS-CONHNH$_2$ and (*S*)-NPX were investigated as a possible drug delivery system – interactions form between the carboxylic acid of (*S*)-NPX and acyl hydrazide functionalised gel fibres of D-DBS-CONHNH$_2$.[21]

Initially, the four combinations of gelator enantiomers, and NPX enantiomers, were investigated. The samples were prepared as before, only with gelator (0.28% wt/vol) and NPX (1 eq.) mixed as solids prior to sonication, heating and cooling. In all combinations, gels formed (Table S6, ESI†). For D-DBS-CONHNH$_2$ with (*R*)-NPX, and L-DBS-CONHNH$_2$ with (*S*)-NPX, the addition of NPX did not have a notable impact on T_{gel}, >100 °C (Table 1). These combinations have an enantiomeric relationship, and should behave the same. The other combinations, D-DBS-CONHNH$_2$ with (*S*)-NPX, and L-DBS-CONHNH$_2$ with (*R*)-NPX, showed a drop in T_{gel} – both below 100 °C (Table 1). Once again these are enantiomeric combinations, however, they have a diastereomeric relationship with the other combinations, and therefore it is logical they may exhibit different physical properties.

In rheology, all the gels showed a clear LVR, but in two specific cases there was variation in stiffness (Fig. S17, S18 and Table S8, ESI†). For D-DBS-CONHNH$_2$, the addition of (*S*)-NPX increased the stiffness (G'), and for L-DBS-CONHNH$_2$ (*R*)-NPX gave an increase. Interestingly, the naproxen enantiomers that decreased thermal stability are those that increase stiffness

Table 1 Comparison of properties of enantiomeric DBS-$CONHNH_2$ gels formulated with enantiomeric forms of naproxen

	Enantiomeric pair		Enantiomeric pair	
Gelator	L	D	D	L
Naproxen	*S*	*R*	*S*	*R*
T_{gel}/°C	>100	>100	98	81
G'/Pa	730	640	1150	1090
% Solid-Like NPX	73	74	68	72

(Table 1). This suggests certain enantiomers stiffen the chiral gel network, decreasing its thermal stability.

^{1}H NMR was used to determine the amount of solid-like NPX, which may be associated with the chiral nanofibers (Table S9, ESI†). There were small differences between enantiomers, with D/*S* and L/*R* systems immobilising slightly less NPX. Although this may suggest differences in the amount of naproxen bound by the gel, these differences are small (Table 1). It seems more likely that the change in gel thermal properties and stiffness results from the different geometries in the different diastereomeric complexes between the gel fibres and NPX.

In summary, we synthesised L-DBS-$CONHNH_2$, investigated its gelation, and compared it to D-DBS-$CONHNH_2$. Mixtures of enantiomers gave weaker gels than the single enantiomers, indicating disruptive interactions. FT-IR suggested these may result from mismatched intermolecular O-H hydrogen bonds. Nanoscale chirality was lost even with addition of only a small proportion of the 'wrong' enantiomer, and TEM indicated the presence of fragmented, poorly defined aggregates in the racemic mixture. The enantiomeric gels were tested for interaction with an enantiomeric carboxylic acid. Although both gels can incorporate both NPX enantiomers, there was an impact on thermal stability and stiffness. This suggested the formation of diastereomeric gel-drug complexes that lead to formulations with different properties. This is the first time the chirality of a DBS gel has been shown to enable enantioselective effects with chiral additives and hints at future potential of DBS systems in applications where chirality is of importance.

Conflicts of interest

There are no conflicts to declare.

Notes and references

1 (*a*) R. G. Weiss, *J. Am. Chem. Soc.*, 2014, **136**, 7519–7530; (*b*) E. R. Draper and D. J. Adams, *Chem*, 2017, **3**, 390–410.
2 (*a*) D. K. Smith, *Chem. Soc. Rev.*, 2009, **38**, 684–694; (*b*) P. Duan, H. Cao, L. Zhang and M. Liu, *Soft Matter*, 2014, **10**, 5428–5448.
3 (*a*) A. R. Hirst, B. Huang, V. Castelletto, I. W. Hamley and D. K. Smith, *Chem. – Eur. J.*, 2007, **13**, 2180–2188; (*b*) B. Adhikari, J. Nanda and A. Banerjee, *Soft Matter*, 2011, **7**, 8913–8922; (*c*) C. Kulkami, J. A. Berrocal, M. Lutz, A. R. A. Palmans and E. W. Meijer, *J. Am. Chem. Soc.*, 2019, **141**, 6302–6309.
4 (*a*) J. Makarević, M. Jokić, Z. Raza, Z. Štefanić, B. Kojić-Prodić and M. Žinić, *Chem. – Eur. J.*, 2003, **9**, 5567–5580; (*b*) D. A. Tómasson, D. Ghosh, Z. Kržišnik, L. H. Fasolin, A. A. Vicente, A. D. Martin, P. Thordarson and K. K. Damodaran, *Langmuir*, 2018, **34**, 12957–12967; (*c*) W. Edwards and D. K. Smith, *Gels*, 2018, **4**, 31.
5 X. Luo, B. Liu and Y. Liang, *Chem. Commun.*, 2001, 1556–1557.
6 (*a*) L. Wang, X. Jin, L. Ye, A.-y. Zhang, D. Bezuidenhout and Z.-g. Feng, *Langmuir*, 2017, **33**, 13821–13827; (*b*) K. McAulay, B. Dietrich, H. Su, M. T. Scott, S. Rogers, Y. K. Al-Hilaly, H. Cui, L. C. Serpell, A. M. Seddon, E. R. Draper and D. J. Adams, *Chem. Sci.*, 2019, **10**, 7801–7806.
7 X. Dou, N. Mehwish, C. Zhao, J. Liu, C. Xing and C. Feng, *Acc. Chem. Res.*, 2020, **53**, 852–862.
8 (*a*) G.-F. Liu, D. Zhang and C.-L. Feng, *Angew. Chem., Int. Ed.*, 2014, **53**, 7789–7793; (*b*) J. Liu, F. Yuan, X. Ma, D. Y. Auphedeous, C. Zhao, C. Liu, C. Shen and C. Feng, *Angew. Chem., Int. Ed.*, 2018, **57**, 6475–6479; (*c*) X. Dou, B. Wu, J. Liu, C. Zhao, M. Qin, Z. Wang, H. Schönherr and C. Feng, *ACS Appl. Mater. Interfaces*, 2019, **11**, 38568–38577.
9 (*a*) G. Liang, Z. Yang, R. Zhang, L. Li, Y. Fan, Y. Kuang, Y. Gao, T. Wang, W. W. Lu and B. Xu, *Langmuir*, 2009, **25**, 8419–8422; (*b*) X. Li, X. Du, J. Li, Y. Gao, Y. Pan, J. Shi, N. Zhou and B. Xu, *Langmuir*, 2012, **28**, 13512–13517.
10 (*a*) F. Rodriguez-Llansola, J. F. Miravet and B. Escuder, *Chem. – Eur. J.*, 2010, **16**, 8480–8486; (*b*) L. N. Neumann, M. B. Baker, C. M. A. Leenders, I. K. Voets, R. P. M. Lafleur, A. R. A. Palmans and E. W. Meijer, *Org. Biomol. Chem.*, 2015, **13**, 7711–7719; (*c*) M. Tena-Solsona, J. Nanda, S. Diaz-Oltra, A. Chotera, G. Ashkenasy and B. Escuder, *Chem. – Eur. J.*, 2016, **22**, 6687–6694; (*d*) K. Hawkins, A. K. Patterson, P. A. Clarke and D. K. Smith, *J. Am. Chem. Soc.*, 2020, **142**, 4379–4389.
11 L. Zhang, Q. Jin and M. Liu, *Chem. – Asian J.*, 2016, **11**, 2642–2649.
12 (*a*) W. Edwards and D. K. Smith, *J. Am. Chem. Soc.*, 2014, **136**, 1116–1124; (*b*) L. Zhang, Q. Jin, K. Lv, L. Qin and M. Liu, *Chem. Commun.*, 2015, **51**, 4234–4236; (*c*) D. Gambhir, S. Kumar, G. Dey, V. Krishnan and R. R. Koner, *Chem. Commun.*, 2018, **54**, 11407–11410; (*d*) X. Xu, L. Qu, J. Song, D. Wu, X. Zhou and H. Xiang, *Chem. Commun.*, 2019, **55**, 9873–9876; (*e*) D. Gambhir, B. Mondal and R. R. Koner, *Chem. Commun.*, 2021, **57**, 2535–2538.
13 B. O. Okesola, V. M. P. Vieira, D. J. Cornwell, N. K. Whitelaw and D. K. Smith, *Soft Matter*, 2015, **11**, 4768–4787.
14 S. Yamasaki, Y. Ohashi, H. Tsutsumi and K. Tsujii, *Bull. Chem. Soc. Jpn.*, 1995, **68**, 146–151.
15 (*a*) B. O. Okesola and D. K. Smith, *Chem. Commun.*, 2013, **49**, 11164–11166; (*b*) B. O. Okesola, S. K. Suravaram, A. Parkin and D. K. Smith, *Angew. Chem., Int. Ed.*, 2016, **55**, 183–187; (*c*) C. C. Piras, P. Slavik and D. K. Smith, *Angew. Chem., Int. Ed.*, 2020, **59**, 853–859; (*d*) C. C. Piras, A. G. Kay, P. G. Genever and D. K. Smith, *Chem. Sci.*, 2021, **12**, 3958–3965.
16 (*a*) R. N. Brogden, R. C. Heel, T. M. Speight and G. S. Avery, *Drugs*, 1979, **18**, 241–277; (*b*) N. Bhala, *et al.*, *Lancet*, 2013, **382**, 769–779.
17 D. J. Cornwell, B. O. Okesola and D. K. Smith, *Soft Matter*, 2013, **9**, 8730–8736.
18 D. J. Adams, *Gels*, 2018, **4**, 32–37.
19 (*a*) B. Escuder, M. Llusar and J. F. Miravet, *J. Org. Chem.*, 2006, **71**, 7747–7752; (*b*) M. Wallace, J. A. Iggo and D. J. Adams, *Soft Matter*, 2015, **11**, 7739–7747; (*c*) S. M. Ramalhete, K. P. Nartowski, N. Sarathchandra, J. S. Foster, A. N. Round, J. Angulo, G. O. Lloyd and Y. Z. Khimyak, *Chem. – Eur. J.*, 2017, **23**, 8014–8024.
20 D. Knani and D. Alperstein, *J. Phys. Chem. A*, 2017, **121**, 1113–1120.
21 (*a*) E. J. Howe, B. O. Okesola and D. K. Smith, *Chem. Commun.*, 2015, **51**, 7451–7454; (*b*) P. R. A. Chivers and D. K. Smith, *Chem. Sci.*, 2017, **8**, 7218–7227; (*c*) A. K. Patterson and D. K. Smith, *Chem. Commun.*, 2020, **56**, 11046–11049.

